

Quark core impact on hybrid star cooling

Rodrigo Negreiros*

FIAS, Goethe University, Ruth Moufang Str. 1 60438 Frankfurt am Main, Germany

V.A. Dexheimer†

Gettysburg College, Gettysburg, USA

S. Schramm‡

CSC, FIAS, ITP, Johann Wolfgang Goethe University, Frankfurt am Main, Germany

(Dated: January 31, 2019)

In this paper we investigate the thermal evolution of hybrid stars, objects composed of a quark matter core, enveloped by ordinary hadronic matter. Our purpose in this paper is to investigate how important is the quark core size to the thermal evolution of the star. In order to do that we use a simple MIT bag model for the quark core, and a relativistic mean field model for the hadronic envelope. By choosing different values for the bag constant (B) we are able to change the phase transition point, which in turn yields hybrid stars with different quark core sizes. We also consider the possibility of color superconductivity in the quark core. Our results indicate that hybrid stars with quark-hadron phase transitions happening between $1.5\rho_0 - 2.0\rho_0$, and with superconductivity gaps (Δ) between 0.1–1.0 MeV are in good agreement with the observed temperature of pulsars.

I. INTRODUCTION

Scientists have been trying to determine the equation of state and composition of compact stars for a long time ([1, 2] and references therein). Many of these studies determine constraints for the equation of state of stellar matter so that the predicted stellar properties agree with the observed masses and radii of pulsars. One of the biggest practical shortcomings of such techniques is the lack of accurate and reliable observations of the radii of compact stars, which makes constraining the equation of state very challenging. A recent paper [3] has put forth unprecedented constraints on the mass-radius diagrams of pulsars, which would certainly make the range of possible equations of state narrower. The analysis of this data however has been questioned [4], and therefore is not universally accepted. Another method that might be used to complement the results provided by the analysis of the structure of the compact star is the examination of the thermal evolution of the object. The cooling of a compact star is intrinsically connected to its microscopic composition, and therefore different microscopic models might lead to different thermal evolutions. The results of the theoretical investigations might then be compared with the wealth of observed data of the thermal properties of compact stars [5, 6]. In this paper we will follow the thermal evolution approach, and with this, probe the composition of compact stars.

In the following we will consider the thermal evolution of hybrid stars, which are objects composed of a strange quark matter core, enveloped by ordinary hadronic matter [1, 2]. The strange quark matter core is composed

of deconfined up, down and strange quarks, as well as electrons that are needed to maintain charge neutrality. The hadronic envelope consists of protons and neutrons, and possibly hyperons (if the chemical potential is high enough); leptons are also present to guarantee charge neutrality and chemical equilibrium. In this work whenever we refer to hybrid stars (HS) we will be referring to objects with a quark core and a hadron envelope; neutron stars (NS) denotes objects made up solely of hadronic matter; and quark stars (QS) refers to stars composed of absolutely stable quark matter. In addition to the equation of state (EoS hereafter) for the quark and hadronic phase, we use the Baym-Pethick-Sutherland (BPS) EoS for the crust of the star[7].

The cooling of neutron stars is dominated by neutrino emissions for the first 1000 years (possibly more for the slow cooling scenario) [8], being replaced by surface photon emission after that. Amongst the neutrino emission mechanisms, the direct Urca (DU hereafter) process sets itself apart by being one of the most efficient ones, with emissivity of the order of 10^{26} erg cm⁻³ s⁻¹ [9]. Due to momentum conservation, the DU process can only take place if the proton fraction is above a certain value. The actual proton-fraction above which the DU process is allowed to take place depends on the underlying microscopic model, and it usually lies between 11%–15%. If a neutron star allows the DU process to take place, the star will exhibit a fast cooling (sometimes also referred to as enhanced cooling). The situation for quark stars is analogous, except that the quark direct Urca process (QDU) [10] is more easily achieved, which causes all quark stars to exhibit an enhanced cooling. The situation is different if pairing in quark matter is considered, since it suppresses the neutrino emission processes and reduces the specific heat of quark matter ([11, 12] and references therein). There is also a plethora of non-trivial thermal processes that might take place inside the com-

* negreiros@fiас.uni-frankfurt.de

† vantoche@gettysburg.edu

‡ schramm@th.physik.uni-frankfurt.de

pact star, and that might change the thermal evolution of the object. Among these are Goldstone bosons decay [13], vortex expulsion [14], and rotochemical heating [15] to name a few. Some of these processes will likely be important to explain the observed high temperature of a few pulsars. We will not, however, consider any of such processes in this work, since we intend to provide benchmark calculations for the cooling of hybrid stars. With such calculations in hand, one will be able to measure deviations introduced by non-standard processes. The neutrino emission channels considered by us in this work are: the direct Urca process [9], the modified Urca process [16] and Bremsstrahlung process [16, 17]. The aforementioned processes take place in the core, and thus we have for each, both the hadron and quark versions. For the crust we consider the electron Bremsstrahlung [18], electron-positron annihilation [19] and plasmon decay [19]. Furthermore we have also included photon emission at the surface of the star.

In this work we will investigate how important the density at which the hadronic matter undergoes a phase transition into quark matter (critical density hereafter) is for the cooling of a hybrid star. We will do that by calculating the cooling of several stars with different EoS. Each EoS has a different critical density. This should provide us with a measure of the importance of the critical density (and equivalently the size of the quark core) for the thermal evolution of hybrid stars. This in turn, might aid us in constraining the EoS for hybrid stars. In order to perform such a study we will use a MIT bag model equation with massive quarks, and first order corrections in α_s , for the quark phase [20–23]. The hadronic EoS will be given by a standard relativistic mean field model with G300 parametrization [1, 24, 25]. These equations of state are relatively simple, and thus represent a good choice for benchmark calculations. In order to obtain different critical densities we vary the values of the bag constant B for the quark matter EoS. With the equations of state calculated we solve the Tolman-Oppenheimer-Volkoff equation to obtain the macroscopic structure of the object, which then allow us to calculate the thermal evolution of the stars. We note that there are more sophisticated models for hybrid stars. See for example [26, 27] where a single model, that accounts for chiral symmetry restoration, is used to describe both the quark and hadron phase, but they allow no control over the critical density.

This paper is organized as follows: in Sec. II we describe the microscopic model used, and present the results for the macroscopic structure of the stars; in Sec. III our results for the thermal evolution of the stars discussed in Sec. II are presented; in Sec. IV the role of superconductivity in the quark core is discussed, and the results for the cooling of superconducting hybrid stars are presented; Finally our final remarks and conclusions can be found in Sec. V.

II. MODEL

For the microscopic model used to describe the hadronic phase, we use a standard relativistic mean field model [1, 2], in which the interactions between the baryons are mediated by the meson fields $(\sigma, \omega, \vec{\rho})$. The parametrization used is G300, which can successfully reproduce the properties of saturated nuclear matter [24].

For the quark matter description we use the MIT Bag Model with massive quarks and first order corrections in the strong interaction coupling constants (α_s) [20–23]. In the framework of the MIT Bag Model, the quarks present at the relevant densities are the up, down and strange. It is important to note, that since we are considering massive strange quarks, electrons are required for charge neutrality to be achieved. At lower densities, the electron population is more significant, due to suppression of the massive strange quarks. This is an important phenomenon, that may lead to the formation of ultra-strong electric fields near the surface of bare strange stars [28–30].

In this work we will also take into account the possibility of color superconductivity. The pattern that will be considered is the Color-Flavor-Locked (CFL from hereafter) [31], where all quarks are paired up. The CFL phase is the most likely condensation pattern at densities $> 2\rho_0$. For intermediate densities ($\sim 2\rho_0$) model calculations seem to indicate that quark matter is in a 2 flavor superconductor state (2SC), where only u and down quarks of two flavors are paired [32]. Another possibility is that quark matter forms a crystalline superconductor, where the momenta of the quark pairs do not add to zero [33, 34].

Since we are considering quark matter only at the inner core of compact stars, we will consider only the CFL phase. It should be noted that one should expect corrections to the quark matter EoS if pairing is considered. Such corrections are $\sim \Delta^2 \mu^2$ [35], and tend to stiffen the EoS. As shown in [35], the effect of color-flavor-locking in the EoS is not extreme, and for the values of Δ considered in this study (0.1 – 10 MeV) they can be safely disregarded. In addition to the quark matter and hadronic matter equation of state, we have also included a crustal EoS, which is given by the Baym-Pethick-Sutherland EoS [7].

The equation of state for the compact star is calculated assuming local charge neutrality and beta equilibrium, as is usual for any bulk system. The phase transition to quark matter is also calculated in the usual way, by connecting the two EoS's at point in which the quark EoS becomes stiffer than the hadronic one (as a function of the baryonic chemical potential). It is our objective to investigate how important the quark-hadron transition is for the cooling of hybrid stars. For that purpose we use different values for the bag constant, which causes the transition to quark matter to take place at different points. This result is shown in Figure 1, where we plot the pressure as a function of energy density for the many

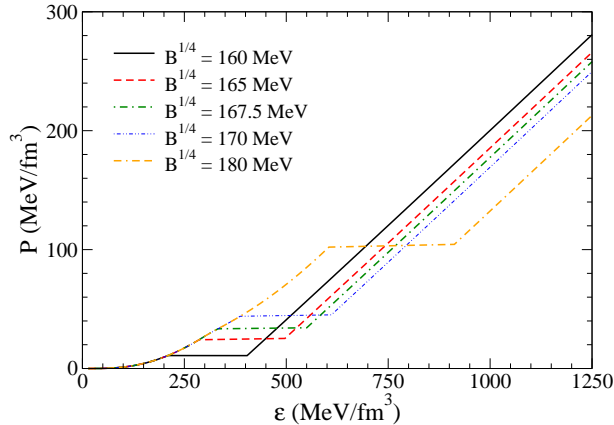


FIG. 1. (Color online) Equation of State for the hadronic and quark phases shown for different bag constants.

bag constants investigated. For values of $B^{1/4} < 160$ MeV, we find that the quark matter is absolutely stable.

The macroscopic properties of the star are obtained by solving the Tolman-Oppenheimer-Volkoff (TOV) equations [36, 37], which are the general relativistic hydrostatic equilibrium equations. Each compact star is uniquely defined by its central density, by changing this quantity continuously one is able to obtain a sequence of stars. Such sequence can be seen in Figure 2, where we show the gravitational mass as a function of radius, for the equations of state shown in Figure 1. The onset of quark matter can be easily identified as the sharp kink found in the sequences. We see that for all values used for the Bag constant, the transition into quark matter yields stable hybrid stars ($\partial M/\partial \rho_c > 0$), except for $B^{1/4} = 180$. This can be understood by analyzing the equation of state shown in Figure 1, where we see that for this value of B the transition into quark matter take place at very high densities, and has a significantly larger density gap. Because of that, all stars with central density above the phase transition are already in the unstable branch of the sequence. Note that for simplicity, we adopt a Maxwell construction of the phase transition. We do not expect any qualitative change of our conclusions if a more elaborate construction were used.

III. RESULTS

We now turn our attention to the thermal evolution of the stars shown in the sequences of Figure 2. The cooling of compact stars is given by the thermal balance

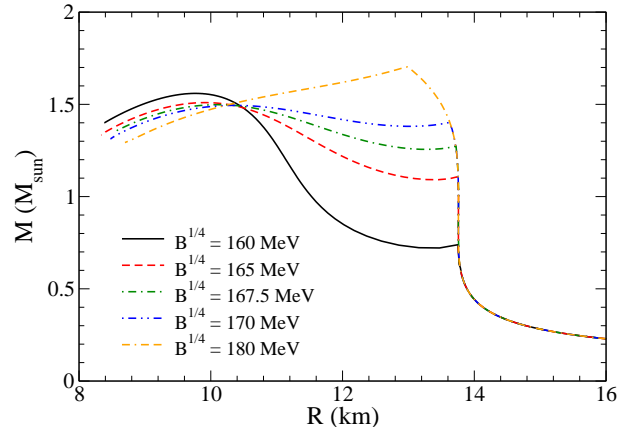


FIG. 2. (Color online) Mass-radius diagram for stars whose equations of state are shown in Figure 1. The sharp kinks denote the phase transition to quark matter. For $B^{1/4} = 180$ MeV the transition to quark matter yields unstable hybrid stars.

and thermal energy transport equation ($G = c = 1$) [1]

$$\frac{\partial(l e^{2\phi})}{\partial m} = -\frac{1}{\rho\sqrt{1-2m/r}} \left(\epsilon_\nu e^{2\phi} + c_v \frac{\partial(T e^\phi)}{\partial t} \right), \quad (1)$$

$$\frac{\partial(T e^\phi)}{\partial m} = -\frac{(l e^\phi)}{16\pi^2 r^4 \kappa \rho \sqrt{1-2m/r}}. \quad (2)$$

In Eqs. 1–2 the structure of the star is given by the variables r , $\rho(r)$ and $m(r)$, that represent the radial distance, the energy density, and the stellar mass respectively. The thermal variables are given by the temperature $T(r, t)$, luminosity $l(r, t)$, neutrino emissivity $\epsilon_\nu(r, T)$, thermal conductivity $\kappa(r, T)$ and specific heat $c_v(r, T)$. The boundary conditions of (1) and (2) are determined by the luminosity at the stellar center and at the surface. The luminosity vanishes at the stellar center since there is no heat flux there. At the surface, the luminosity is defined by the relationship between the mantle temperature and the temperature outside of the star [8, 12, 38, 39].

In order to investigate the importance of the phase transition point, we chose two stars for each sequence shown in Figure 2. These are the maximum mass star, and the maximum mass star before the phase transition into quark matter. The properties of these objects can be found in Table I

The cooling of the objects described in Table I is shown in Figures 3 - 5, that shows the redshifted temperature as a function of the age of the star. We have also plotted some prominent observed temperatures for a few pulsars. These data are separated into two sets. The first set, labeled spin-down, contains the temperature of objects whose age are estimated based on their spin-down age. The second set, labeled kinematic, consists of age estimates based on the observed movement of the object

TABLE I. Stellar properties of a few objects from the sequences displayed in Figure 2. These stars are used for the thermal evolution investigation. All symbols have their usual meaning, and R_q denotes the radius of the quark matter core.

$B^{1/4}$ (MeV)	ϵ_c (MeV/fm ³)	R_q (km)	R (km)	M (M_\odot)
160.0	203.46	0.0	13.90	0.75
	1465.28	8.29	10.02	1.55
165.0	286.0	0.0	13.75	1.10
	1512.51	7.4	10.22	1.50
167.5	332.0	0.0	13.72	1.27
	1536.0	6.99	10.39	1.49
170.0	386.0	0.0	13.65	1.37
	1561.0	6.55	10.56	1.49

with respect to its progenitor supernova remnant. A detailed discussion about the observed data can be found in references [5, 6].

Analyzing Figure 3 we can see that stars with low masses, which implies small quark cores, are in better agreement with the observed data. In this case, as shown in Figure 1, the phase transition occurs at a relatively low density, and therefore the hadron envelope is constrained to the low density regime. This implies that the hadron direct Urca process is not allowed to happen, which causes the star to exhibit a slow cooling. As the central density of the star increases, the critical density is reached, and the star develops a quark matter core. In the high density core, the quark direct Urca process is allowed to take place and the star presents a faster cooling. The situation is qualitatively the same for the case in which $B^{1/4} = 165$ MeV, as shown in Figure 4.

For stars with $B^{1/4} = 167.5$ and 170 MeV the situation is different. In these cases, the phase transition occurs at higher densities, which allows the hadron envelope to reach higher densities. The densities reached at the hadronic layer permit the direct Urca process to take place, hence even stars with $R_q = 0.0$ km display a fast cooling, as shown in Figure 5. The situation is the same for $B^{1/4} = 170$ MeV, and thus we omit the figure for this case.

These results seem to indicate that a compact star needs to have a small or no quark core at all to be in agreement with the observed thermal data (if only standard cooling mechanisms are considered). This situation is different if pairing in the quark matter is considered, as we will show in next section.

IV. ROLE OF COLOR SUPERCONDUCTIVITY

As mentioned in section II, strange quark matter is expected to be in a superconducting phase. The most likely condensation pattern for high densities is the Color-Flavor-Locked state, in which all quarks are paired. Because of the pairing the direct Urca process is suppressed by a factor $e^{-\Delta/T}$, and the modified Urca and the

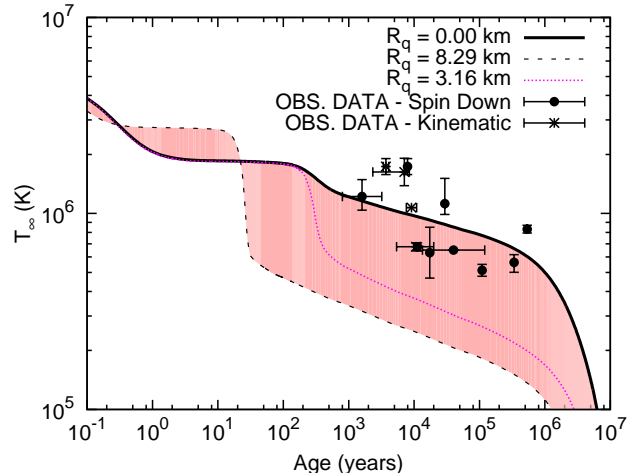


FIG. 3. (Color online) Cooling of hybrid stars with $B^{1/4} = 160$ MeV. T_∞ denotes the temperature observed at infinity, and the x axis the age in years. The top (lower mass) and bottom (higher mass) curves represent the cooling of the stars described in Table I. The cooling of an intermediate mass star is also plotted for comparison. Two sets of observed data were used, one whose age estimate is based on spin-down rate, and another that is based on the kinematic age [5, 6].

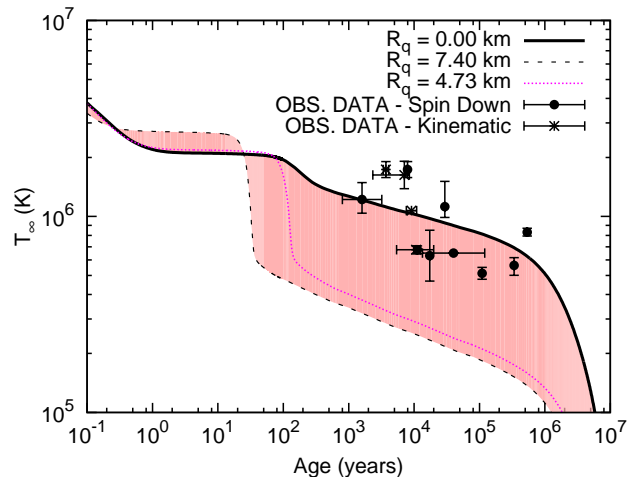


FIG. 4. (Color online) Same as Figure 3, but for $B^{1/4} = 165$ MeV.

Bremsstrahlung processes by a factor $e^{-2\Delta/T}$, for $T \leq T_c$, where Δ is the gap parameter for the CFL phase and T_c is the critical temperature below which strange matter undergoes a phase transition into CFL matter. In addition to changes in the neutrino emissivities, the specific heat of quark matter is also modified, being reduced by the factor $3.2(T_c/T) * (2.5 - 1.7(T/T_c) + 3.6(T/T_c)^2)e^{-\Delta/T}$. For our calculations we have used $T_c = 0.4\Delta$.

We now show in Figures 6 - 7 the results for the cooling

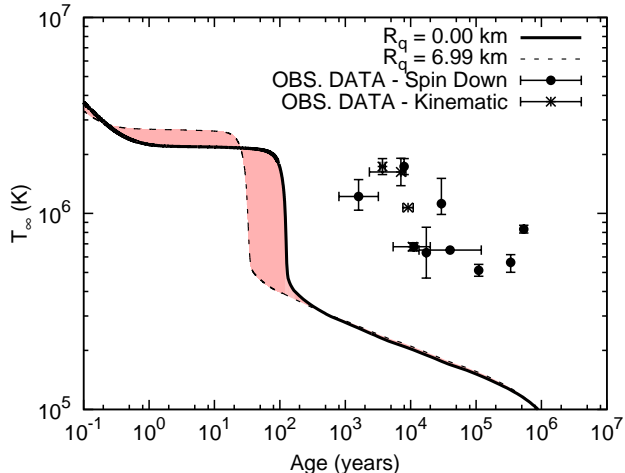


FIG. 5. (Color online) Same as Figure 4, but for $B^{1/4} = 167.5$ MeV.

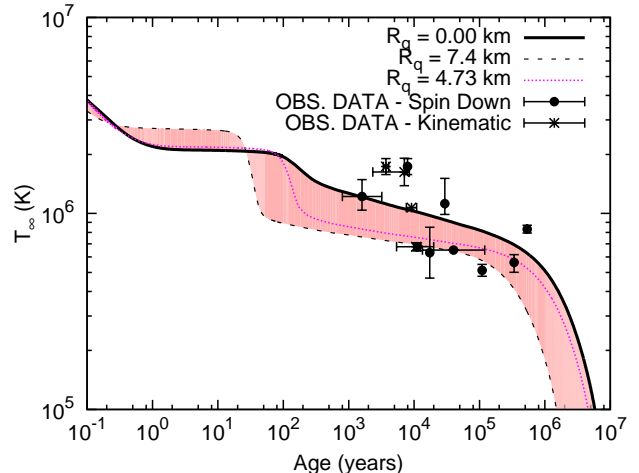


FIG. 7. (Color online) Same as Figure 6 but for $B^{1/4} = 165$ MeV.

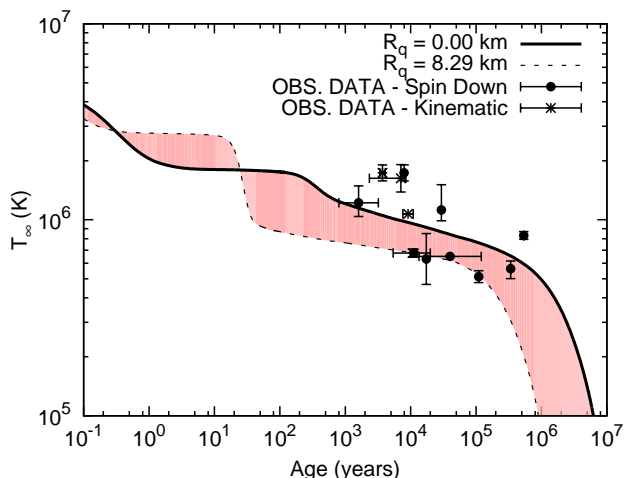


FIG. 6. (Color online) Cooling of hybrid stars with $B^{1/4} = 160$ MeV, and $\Delta = 0.1$ MeV. T_{∞} denotes the temperature observed at infinity. The top and bottom curves represents the critical stars described in Table I. Two sets of observed data were used, one whose age estimate is based on spin-down rate, and another that is based on the kinematic age [5, 6].

of hybrid stars, whose quark core is composed of strange quark matter in the CFL phase with $\Delta = 0.1$ MeV.

Figures 6 - 7 show us that if the strange matter core is in the CFL phase, the fast cooling exhibited by stars with higher masses is slowed down. This effectively narrows the band shown in Figures 3 - 4. The reason for that is the suppression of the quark emission processes. Furthermore, since in the cases depicted in Figures 6 - 7 ($B^{1/4} = 160$ and 165 MeV) the hadron envelope does not allow the hadron Urca process, the overall cooling of the star is slowed down. For the case in which $B^{1/4} = 167.5$

MeV (and equivalently 170 MeV) the situation is the same as for the non-superconducting quark cores, since in these cases the hadron envelope allows the hadron Urca process, which then dominates the cooling keeping the overall behavior unchanged. For that reason we omit the graphs displaying these results.

It is also important to estimate the importance on the gap parameter Δ to the cooling, since a higher value for this constant will strengthen the suppression of the neutrino emission processes. In order to do that we have calculated the cooling of hybrid stars with $\Delta = 10.0$ MeV. These results are shown in Figure 8-9, and as expected the stronger suppression of the neutrino emissivity shrinks even more the bands shown in Figures 3 - 4. Furthermore the cooling in the quark core becomes so slow, that for intermediate ages (between $10^2 - 10^5$ years) the temperature of the maximum mass star is higher than the purely hadronic star. For higher values of the bag constant ($B^{1/4} = 167.5$ MeV and higher) the situation is the same as the other cases analyzed, with the direct Urca process in the hadron envelope dominating the thermal evolution and causing a fast cooling.

For values of $\Delta > 10$ MeV, we have found that the thermal evolution is essentially the same as for $\Delta = 10$ MeV. This is easy to understand, considering that the suppression factor goes with the exponential of $-\Delta/T$, and the fact that for the relevant ages (> 0.1 year) the temperature of the star is of the order of $10^{-2} - 10^{-3}$ MeV. This implies that the exponential $\exp(-\Delta/T)$ is essentially zero $\Delta > 10$ MeV and at the ages relevant to this study.

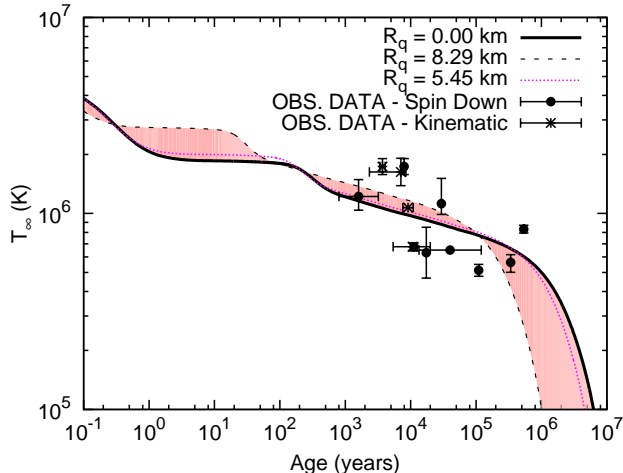


FIG. 8. (Color online) Cooling of hybrid stars with parameters $B^{1/4} = 160$ MeV, and $\Delta = 10$ MeV. T_∞ denotes the temperature observed at infinity. The top and bottom curves represent the stars described in Table I. Two sets of observed data were used, one whose age estimate is based on spin-down rate, and another that is based on the kinematic age [5, 6].

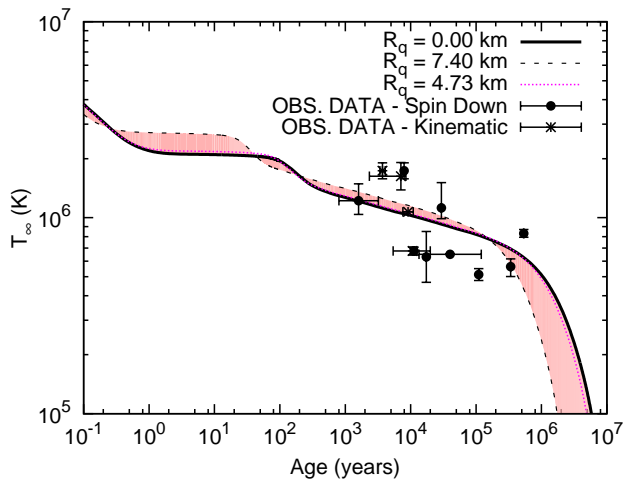


FIG. 9. (Color online) Same as Figure 6 but for $B^{1/4} = 165$ MeV.

V. DISCUSSION & CONCLUSIONS

It is the purpose of this paper to investigate the importance of the critical density in the quark-hadron phase transition, to the thermal evolution of hybrid stars. Even though there has been many papers analyzing different models for hybrid stars, and how well they agree with observational mass and radius constraints [26, 27, 40, 41], we intend to provide a complementary study, in which observed temperatures of pulsars, together with cooling simulations of hybrid stars are used to infer the impor-

tance of the critical density (and therefore the size of the quark matter core) on the thermal evolution. To achieve that we have used a MIT bag model for the quark phase, and a relativistic mean field model with parameterization G300 for the hadron phase. Different values for the bag constant (B) were used, which lead to different critical densities, and thus different structures and quark core sizes. Values of $B^{1/4} < 160$ MeV yields absolutely stable quark matter which indicates no phase transition to hadron matter. $B^{1/4} > 170$ yields very high critical densities (see Figure 1), which causes the stars with a quark core to be in the unstable branch of the mass-radius diagram, as shown in Figure 2. In this study we also consider the possibility of color superconductivity in the quark core. The condensation pattern considered by us is the Color-Flavor-Locked. If the quark core is in a superconductor state, the neutrino emission processes as well as the specific heat will be suppressed, thus modifying the thermal evolution of the star.

Our results were compared to a set of prominent observed data for the thermal properties of a few pulsars. There were two sets of data used, one whose age was based on the spin-down rate of the star (labeled spin-down), and another whose age estimate is based on the motion of the pulsar with respect to its originating supernova remnant (labeled kinematic). By comparing our results to this data we are able to measure the quality of models with different properties (quark core sizes and gap parameters).

For the values of B investigated, we have found that for $B^{1/4} = 160$ and 165 MeV, the phase transition to quark matter takes place at relatively low densities ($\epsilon = 200 - 300$ MeV/fm³). This leads to relatively large quark cores, and limits the hadron envelope to lower densities. Because of this low density, the hadron direct Urca process is not allowed to take place in the hadronic phase. Hence, stars dispossessed of a quark core (stars with low central density) will exhibit a slow cooling. For more massive stars, that have higher central density, a quark core is present. The direct Urca process is more easily achieved in quark matter, and thus as the quark core increases (for higher mass stars) the cooling of the star becomes correspondingly faster, as shown in Figures 3 and 4. For $B^{1/4} = 167.5$ MeV, the phase transition to quark matter happens at a higher density, and the hadronic envelope can attain higher densities. In this case, differently than for the low values of B , the direct Urca process is present in the hadron envelope. This causes the objects with no quark core to exhibit a fast cooling as well, and in the event that a quark core is present the cooling is further enhanced, as shown in Figure 5. The situation is the same for $B^{1/4} = 170$ MeV, except that the quark cores are slightly bigger. These results seem to favor hybrid stars with a low critical density, since high values would lead to fast cooling that is in disagreement with the observed data. It should be noted that even for low critical densities, the observed data is better represented by stars with a small quark cores. As shown in

Figure 3, objects with a quark core bigger than 1.45 km exhibit a temperatures well below the observed data.

The situation changes considerably if pairing is turned on. As mentioned before, in the event that the quark core is in a superconductor state, the neutrino emission processes are suppressed and one would expect the cooling to be slower. This is indeed the case, as can be seen in Figures 6 and 7, where the cooling of hybrid stars, with quark cores in the CFL phase with $\Delta = 0.1$ MeV is shown. In the cases depicted in these figures, the hadron envelope does not allow for the direct Urca process, and thus with the neutrino emissivities suppressed in the quark core, the overall cooling is slowed down. This effectively reduces the band shown in Figures 3–4. For $B^{1/4} \geq 167.5$ MeV, the situation is qualitatively the same as the non-superconducting case. The reason for that is that the direct Urca process takes place in the hadron envelopes, which then dominates the cooling. Hence, even with the neutrino emissivities suppressed in the quark core, the star still exhibits a fast cooling.

Finally we investigated the cooling of hybrid stars with CFL quark cores, whose gap parameter is $\Delta = 10$ MeV. For this value of Δ the suppression of the neutrino emission processes is stronger, and the cooling band is even more narrow. In this case, the cooling of the quark core becomes so slow, that the temperatures of hybrid stars is higher than that of purely hadronic stars (for ages between $10^2 - 10^5$ years), as shown in Figure 8–9. For higher values of B ($B^{1/4} > 167.5$ MeV), the situation is analogous to the other cases investigated, with the hadronic direct Urca process dominating the cooling, and making quark pairing irrelevant for the thermal evolution. We have also investigated the cooling of stars with $\Delta > 10$ MeV, and have found that the results are almost the same as for the case in which $\Delta = 10$ MeV, with slight differences for very early ages ($< 10^{-1}$ year). This can be easily understood by taking into account the temperature of the star in the relevant ages, which is $\sim 10^{-2} - 10^{-3}$ MeV. In this case, the suppression factor $\exp(-\Delta/T)$ saturates for ages relevant to this study.

The results presented here indicate that it is possible to explain the observed thermal properties of pulsars with a hybrid star model. Clearly, some of the observed data shown in this paper did not fit the theoretical predictions, having a higher temperature than that predicted. This situation however is present in studies involving ordinary

neutron stars (i.e. with no pairing or exotic thermal processes) as well, and thus this mismatch should not be attributed to the underlying hybrid star model, but probably to some non-standard thermal process taking place in these objects. Furthermore, the results we obtained that best represented the observed data, were the ones for hybrid stars with a CFL quark core with $\Delta = 0.1$ MeV, and with $B^{1/4} \leq 165$ MeV. In other words, it appears that a hybrid star, whose phase transition to quark matter takes place at a relatively low density $\sim 1.5\rho_0 - 2.0\rho_0$, and whose quark core is in a CFL superconductor state with small gaps, give the better description of the observed data points analyzed. A higher critical density allows the hadronic envelope to attain higher densities, which in turn allows the hadron direct Urca process to take place. In this case, the aforementioned process dominates the cooling, rendering any superconducting suppression of quark processes irrelevant, which leads to a fast cooling that is in disagreement with the observed data. For higher values for the gap parameter ($\Delta \geq 10$ MeV), the band of possible cooling curves becomes too narrow, and almost independent of the mass of the star, and in this case only a few of the observed data can be explained, with others falling below the predicted band.

It is important to remember that the model considered by us in this paper is somewhat simple. A more realistic study, considering for example different degrees of freedom and chiral symmetry restoration [26, 27, 41] would certainly be of interest. Work in that line is currently in progress. Nevertheless it seems clear to us that regardless of the microscopic model used to describe the quark and hadronic phase, our results and conclusions would still hold. The change in composition among different microscopic models is, most likely, not big enough to alter the conclusions drawn in this paper. This is not to say that exotic microscopic processes will not change the thermal evolution. Some processes not considered in this paper would most likely alter the cooling. Amongst these processes not investigated, we believe that pairing in the hadronic phase will play an important role for the cooling of hybrid stars, and we intend to perform a similar investigation in the future, considering this phenomenon. It seems clear to us however, that for a hybrid star model to agree with observed data, it will need to have a relatively low critical density and small values for the superconductivity gap parameter ($\Delta = 0.1 - 1$ MeV).

[1] F. Weber, *Pulsars as astrophysical laboratories for nuclear and particle physics*, 1st ed. (Institute of Physics, Bristol, 1999).
 [2] N. K. Glendenning, *Compact stars : nuclear physics, particle physics, and general relativity*, 1st ed. (Springer, 2000).
 [3] F. Ozel, G. Baym, and T. Guver, arXiv:1002.3153v1 (2010).
 [4] A. W. Steiner, J. Lattimer, and E. F. Brown,

arXiv:1005.0811v2 (2010).
 [5] D. Page, J. Lattimer, M. Prakash, and A. W. Steiner, *The Astrophysical Journal Supplement Series* **155**, 623 (2004).
 [6] D. Page, J. Lattimer, M. Prakash, and A. W. Steiner, *The Astrophysical Journal* **707**, 1131 (2009).
 [7] G. Baym, C. Pethick, and P. Sutherland, *The Astrophysical Journal* **170**, 299 (1971).
 [8] D. Page, U. Geppert, and F. Weber, *Nuclear Physics A*

- 777, 497 (2006).
- [9] J. Lattimer, C. Pethick, M. Prakash, and P. Haensel, *Physical review letters* **66**, 27012704 (1991).
- [10] N. Iwamoto, *Annals of Physics* **141**, 1 (1982).
- [11] J. Horvath, O. Benvenuto, and H. Vucetich, *Physical Review D* **44**, 3797 (1991).
- [12] D. Blaschke, T. Klahn, and D. Voskresensky, *The Astrophysical Journal* **533**, 406412 (2000).
- [13] P. Jaikumar, M. Prakash, and T. Schäfer, *Physical Review D* **66**, 1 (2002).
- [14] B. Niebergal, R. Ouyed, R. Negreiros, and F. Weber, *Physical Review D* **81**, 043005 (2010).
- [15] C. Petrovich and A. Reisenegger, arXiv:1002.5043v1.
- [16] B. Friman and O. Maxwell, *Astrophysical Journal* **232**, 541 (1979).
- [17] O. V. Maxwell, *The Astrophysical Journal* **231**, 201 (1979).
- [18] A. D. Kaminker, C. J. Pethick, A. Y. Potekhin, V. Thorsson, and D. G. Yakovlev, *Astronomy and Astrophysics* **343**, 1009 (1999).
- [19] D. Yakovlev, *Physics Reports* **354**, 1 (2001).
- [20] A. Chodos, R. Jaffe, K. Johnson, C. Thorn, and V. Weiskopf, *Physical Review D* **9**, 3471 (1974).
- [21] A. Chodos, R. Jaffe, K. Johnson, and C. Thorn, *Physical Review D* **10**, 2599 (1974).
- [22] E. Farhi and R. Jaffe, *Physical Review D* **30**, 2379 (1984).
- [23] F. Weber, *Progress in Particle and Nuclear Physics* **54**, 193 (2005).
- [24] N. Glendenning, *Nuclear Physics A* **493**, 521 (1989).
- [25] R. Picanco Negreiros, *Numerical study of the properties of compact stars*, Ph.D. Thesis, San Diego State University (2009).
- [26] R. Negreiros, V. Dexheimer, and S. Schramm, *Physical Review C* **82**, 035803 (2010).
- [27] V. A. Dexheimer and S. Schramm, *Physical Review C* **81**, 045201 (2010).
- [28] C. Alcock, E. Farhi, and A. Olinto, *The Astrophysical Journal* **310**, 261 (1986).
- [29] V. Usov, *Physical Review D* **70**, 14 (2004).
- [30] R. Negreiros, F. Weber, M. Malheiro, and V. Usov, *Physical Review D* **80**, 083006 (2009).
- [31] M. Alford, *Annual Review of Nuclear and Particle Science* **51**, 131 (2001).
- [32] M. Alford, A. Schmitt, K. Rajagopal, and T. Schäfer, *Reviews of Modern Physics* **80**, 1455 (2008).
- [33] M. Alford, J. Bowers, and K. Rajagopal, *Physical Review D* **63**, 074016 (2001).
- [34] J. Bowers and K. Rajagopal, *Physical Review D* **66**, 065002 (2002).
- [35] G. Lugones and J. E. Horvath, *Physical Review D* **66**, 074017 (2002).
- [36] R. Tolman, *Physical Review* **55**, 364 (1939).
- [37] J. Oppenheimer and G. Volkoff, *Physical Review* **55**, 374 (1939).
- [38] E. H. Gudmundsson, C. J. Pethick, and R. I. Epstein, *The Astrophysical Journal* **259**, L19 (1982).
- [39] E. H. Gudmundsson, C. J. Pethick, R. I. Epstein, *The Astrophysical Journal* **272**, 286 (1983).
- [40] A. Kurkela, P. Romatschke, A. Vuorinen, and B. Wu, arXiv:1006.4062v1 (2010).
- [41] D. Blaschke, J. Berdermann, and R. Lastowiecki, arXiv:1009.1181v1 (2010).